BNL 39091
INFORMAL REPORT

BNL--39091

DE87 004176

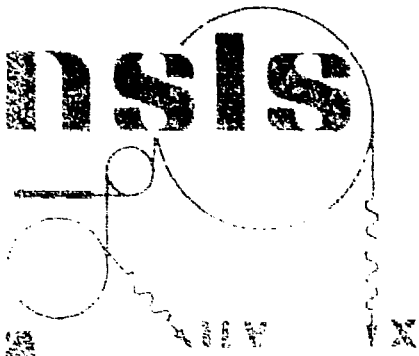

ANALYSIS OF SURFACE CONTAMINANTS ON BERYLLIUM WINDOWS

NICHOLAS F. GMUR

DECEMBER 1986

NATIONAL SYNCHROTRON LIGHT SOURCE

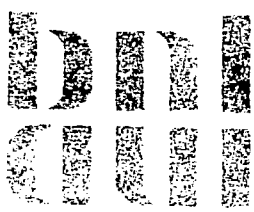

BROOKHAVEN NATIONAL LABORATORY
ASSOCIATED UNIVERSITIES, INC.
Under Contract No. DE-AC02-76CH00016 with the
UNITED STATES DEPARTMENT OF ENERGY

BNL 39091
INFORMAL REPORT

ANALYSIS OF SURFACE CONTAMINANTS ON BERYLLIUM WINDOWS

Nicholas F. Gmur

December 1986

DISCLAIMER

Research Supported by the
OFFICE OF BASIC ENERGY SCIENCES
U.S. Department of Energy
Washington D.C.

NATIONAL SYNCHROTRON LIGHT SOURCE
BROOKHAVEN NATIONAL LABORATORY
Associated Universities, Inc.

Under Contract No. DE-AC02-76CH00016

TABLE OF CONTENTS

I. INTRODUCTION

Current policy[1] at the National Synchrotron Light Source (NSLS) dictates that beryllium windows mounted on x-ray beam lines may not exist with their downstream faces exposed to air. These downstream faces must be protected by a further beam pipe section either under rough vacuum or containing a helium atmosphere which is itself "capped" by a non-beryllium window such as Kapton (3M Corporation, St. Paul, MN) or aluminum. This policy is in force due to the fact that in the presence of a full-spectrum, i.e., white, synchrotron radiation (SR) beam, substances will form on the downstream surface of the beryllium window exposed to air which might (a) endanger the health of the attendant researcher and/or (b) might endanger the vacuum integrity of the beam line and therefore the storage ring vacuum.

It is known (personal communication W. Thomlinson, NSLS; G. Materlik, HASYLAB; J. Cerino, SSRL) that various crystalline and liquid compounds form on the downstream surfaces of beryllium windows exposed to air. It is also known (personal communication L.D. Chapman, NSLS) that the integrity of such windows may be compromised resulting in leaks through the window. The purpose of this report is to document the occurrences described above as they pertain to the NSLS and to analyze, where possible, the various substances formed.

II. BERYLLIUM WINDOWS STUDIED FOR THIS REPORT

The beryllium windows used on NSLS beam lines are purchased from a number of sources such as Brush Wellman, Inc. in Cleveland, Ohio and Electrofusion Corporation in Menlo Park, California. A typical window is a circular disk 1.5 inches in diameter and 0.010 inches thick, and is of high purity (see Table 1).

Table 1. Material Test Report for High Purity (99.8%) Beryllium Ingot Foil, Vacuum Tight, 0.010" x 1.5" diameter (Electrofusion Corporation, Menlo Park, California; dated October 18, 1985)

Be assay	99.86 %	BeO	< 60 ppm
Fe	65 ppm	Al	< 20 ppm
Mg	7 ppm	Si	< 20 ppm
C	210 ppm	Cr	< 10 ppm
Co	< 10 ppm	Cu	10 ppm
Pb	< 1 ppm	Mn	4 ppm
Mo	< 10 ppm	Ni	83 ppm
Ca	< 200 ppm	Zn	< 100 ppm
Ag	< 1 ppm	Ti	< 10 ppm

The particular windows studied in this report are described in the following subsections.

A. Type A Beryllium Window

During the NSLS x-ray ring commissioning period, each beam line front end section (consisting at that time of a water-cooled mask and a gate valve) was sealed at its downstream end by a beryllium window exposed to UHV on its upstream face and air on its downstream face. A white SR beam of x = 16 mm and y = 4.5 mm dimensions as measured by the carbon deposit on the upstream window face generated a downstream face deposit of x = 16 mm and y = 2 mm dimensions (see Fig. 1). This deposit typically consisted of a narrow white crystalline mid-portion surrounded by a very thin shiny lacquer-type layer which was hard, clear and slightly yellow in color (see Fig. 2). Another variation was a window with only the thin shiny lacquer deposit (see Fig. 3). Conditions during this commissioning period (personal communication Paul Cowan) were approximately as follows: ring energy 1.7 GeV, ring current < 5 mA, length of beryllium window exposure to photon beam < 5 hours.

B. Type B Beryllium Window

In May 1986, a condition arose on a white x-ray beam line which created this type of window surface deposit. A circular (1.5" diameter) window was mounted in the beam line at 13,182 mm from the dipole magnet source. Another pipe section was mounted downstream of the window. This pipe was, as per regulations, filled with He gas at atmospheric pressure and was capped by a Kapton window. Typically, the Kapton window was replaced once a week, but in this situation it was not and the SR beam burned a hole through it. The He gas leaked out of the pipe section (it was not replaced by the associated He supply system) and air entered the pipe. This condition continued for 48-72 hours with SR beam at which point the damage was discovered. The resulting deposit which formed on the downstream face of the beryllium window (see Fig. 4) was a thin white powdered area (x = 13.3 mm, y = 2.5 mm) similar to the dimensions of the incoming beam. Figure 5 is an 80x image of the upper edge of the white powder area on the beryllium surface. Figure 6 is a 25x image of the end of the deposit (side is away from the ring) and also shows the result of accumulated deposits due to three different horizontal aperture settings (A = narrowest --> C = widest).

C. Type C Beryllium Window

In August 1986, a vacuum leak was detected on an x-ray beam line in the area where the white SR beam struck a beryllium window sealing the upstream aperture to the monochromator box. Upon disassembly and removal of the beryllium window (x = 4.0", y = 0.75") from its copper mount, the downstream face of the window (facing into the He atmosphere of the monochromator) was found to be heavily covered with areas of white powder, blue/green opaque gel, white semi-translucent gel, orange crystals and pits into the surface of the window (see Fig. 7-10). Upon further examination, it was discovered that the water cooling system incorporated into the window's copper mount had leaked and water had condensed onto the downstream face of the window. Also found by using a 20x dissecting microscope was that some of the pits formed on the window surface went clear through to the upstream face, hence the vacuum leak. It is not clear how long the window had been exposed to the water (perhaps on the order of months). The most severe pitting and orange crystal formation was located along that line on the window surface where the rubber O-ring (used to seal the window in its copper mount) and the SR beam interacted along with, one assumes, the water.

III. ANALYSIS OF BERYLLIUM WINDOW SURFACE DEPOSITS

A. White Powder/Crystal Deposits

An initial attempt was made to analyze the white powder formed on beryllium windows in-situ without attempting to remove the powder from the window surface. This was done because the powder layers on type A and B windows were so thin as to be virtually impossible to remove without scratching the window surface itself, thus contaminating the sample. A spectroscopic analysis was, therefore, made by sparking the window surfaces at the location of the powder (see Fig. 7). The results are given in Table 2.

Table 2. Results of Spectroscopic Analyses by Sparking of Beryllium Window Surfaces
(DAS - Analytical Laboratory; Dated August 5, 1986)

Window Type	Elements Analyzed						
	Mg	Si	Cu	Pb	Mo	Ag	Be
A	Trace[b]	Trace	Trace	N.D.	Trace	Trace	Major
(A)[a]	(Trace)	(N.D.)	(Trace)	(N.D.)	(Trace)	(N.D.)	(Major)
B	Trace	Trace	Trace	N.D.	Trace	N.D.	Major
C	Trace	Trace	Minor	Trace	Minor	N.D.	Major

a. Type A window with lacquer deposit only.
b. Relative order of elemental concentrations:
N.D.(not detectable) -> Trace -> Minor -> Major

While the presence of copper on the C window may confirm subsequent work, the results given above are generally not very useful. All of the above elements are found as contaminants in the beryllium windows (see Table 1). It is also evident from the sparking area (see Fig. 7), typically 8 mm in diameter and penetrating the window to some depth, that not just the surface deposits were being analyzed. This coarse method of analysis was thus abandoned.

Further analysis of the white powder was attempted by x-ray diffraction using a Debye-Scherrer Camera. A 40 keV, 30 mA electron beam was directed at a copper target with a nickel filter resulting in a monochromatized photon beam peaking at 8.3 keV. Clean, dry white powder was collected in a 0.3 mm I.D. glass capillary tube from the surface of the C-type window for this analysis. The results of the analysis (personal communication R. Sabatini, DAS) were as follows:

> "The x-ray diffraction did not supply any useful information. The pattern on the film turned out to show just a broad diffuse band and a few strong reflections which were analyzed as Fe (probably an impurity introduced in handling of the sample)."

Also using window type C white powder, a final successful attempt at analysis was made using the facilities of a JEOL JEM-100C Transmission Electron Microscope (TEM) operating at a 120 keV accelerating voltage. In the electron diffraction mode, the ring pattern produced consisted of both diffuse as well as distinct rings indicating a mixture of amorphous and microcrystalline phases (see Fig. 11). As calculated, ring diameters corresponded to d-spacings of 2.28 Å, 1.62 Å, 1.37 Å and 1.18 Å which in turn were interpreted (R. Sabatini - DAS) to be representative of beryllium oxide - BeO (see Fig. 12). This finding was supported by electron energy loss spectroscopy (EELS - using a Gatan Energy Loss Spectrometer, Model 607, with a serial type detector) which detects the electron energies resulting from the interaction of the electron beam as it passes through the sample. The spectra clearly show the presence of beryllium (peak at 111 eV) and oxygen (peak at 532 eV), (see Fig. 13,14). Finally, the imaging mode of the TEM caused the fine mass of powder to charge up in the presence of the electron beam indicating the powder is an insulator. All of these factors, confirmed in the literature[2-5] indicate that the powder is BeO.

The mode of formation of the BeO is conjectured to be due to the action of the SR beam with the water condensed in that region of the type C window. Since the window was exposed to vacuum on its upstream face and to helium on its downstream face, the oxygen probably came from the ionization of the water. The elemental oxygen then reacted with the beryllium to form BeO. This would also be the case in window surfaces exposed to air. This surface reaction is probably accelerated to some extent due to the localized formation of ozone by the SR beam. It is also possible that an air leak existed at this location, but none was detected at the time of the removal of the window from the beam line.

From a health risk perspective, the beryllium oxide powder is perhaps more dangerous than beryllium metal due to the fact that the powder may be released into the local atmosphere if the surface of the window is disturbed. Current exposure limits are set by the Occupational Safety Health Administration (OSHA) to be 2 $\mu g/m^3$ (8 hr. time-weighted average over a 40 hour work week) with a ceiling concentration of 5 $\mu g/m^3$. The maximum peak above the acceptable ceiling concentration/8 hour shift is 25 $\mu g/m^3$ for a maximum duration of 30 minutes.[2,6]

B. Gel Deposits

Liquid deposits have been mentioned as occuring on beryllium window surfaces. During this series of analyses, no liquids per se were ever found on windows. However, two related phases were observed. On type A windows, to either side of the narrow line of powder, a very thin lacquer-like substance was deposited (see Fig. 2). This substance was clear, slightly yellow in color and very hard when touched with fine forceps. Its thinness and hardness precluded any way of obtaining an uncontaminated sample. The yellow color may indicate that the substance is some form of nitrate.

The type C window exhibited large areas where gels had formed. The gels were located mainly on the areas where the rubber O-ring pressed against the downstream beryllium window surface. Two forms of gel were present: (a) white semi-translucent and (b) opaque milky blue/green (see Figs. 8,9).

Both gels were very viscous and extremely hard to sample. It was thought at one point that the gels were some form of deliquescent beryllium compound. This theory was dispelled after the window was placed in a dessicating jar (approximately 0% RH) for 7 days and the gels remained unchanged. Moeller (1952) confirmed the absence of the deliquescence property in BeO. The white gel was determined to be mainly amorphous carbon based on electron diffraction and EELS analyses (see Figs. 15,16). The EELS analysis exhibited the π^* feature which is characteristic of the carbon edge at 284 eV. Carbon was also found in the blue/green gel. This finding is a source of confusion because carbon, much less in a gel form, was not expected. The literature is somewhat confused regarding the presence[2] or absence[3-5,10] of a gel form of BeO. Experts in the field were consulted (B. Hill, Chief of R&D, Brush Wellman, Inc.; R. Stoenner, Chemistry Dept., BNL: R. Weast, Editor-in-Chief, 66th Edition of CRC Handbook of Chemistry and Physics). Not one of these individuals was familiar with a BeO gel. In this current set of analyses, Be was not found in either gel type. The conjecture at this point, therefore, is that the presence of the carbon gel may be due to the interaction of the SR beam with the rubber O-rings and/or lubricant used to seal the window/copper mount assembly onto the monochromator box.

Also present in the blue/green gel were metallic copper and Cu_2O as determined from electron diffraction and EELS patterns (see Fig. 17-20). While copper is present as a trace contaminant of beryllium (see Table 1), it is more likely that the copper found in this gel was somehow leached from the mirror mount which was also made of copper.

C. Orange Crystals

As detailed above, orange crystals were found only on the type C window in the area where the SR beam, the O-ring and the copper mount converged (see Fig. 7,10). Obtaining uncontaminated samples in this area for electron diffraction and EELS analyses was made difficult by the fact that the crystals were in a sense glued to their Be substrate which in turn had lost some of its hardness in this area and had been rendered very heavily viscous (similar to the gels) by action with the SR beam. The diffraction pattern (see Fig. 21) exhibits spotty rings akin to metallic copper as well as weak discontinuous rings related to Cu_2O (see Fig. 18). The EELS analysis confirmed the presence of copper and oxygen. The evidence of the M_1 copper edge at 121 eV was further confirmed by the L_2 and L_3 copper edges at 931 and 951 eV, respectively (see Fig. 22). Also found in this sample by EELS was the additional presence of carbon with the π^* edge feature (see Fig. 23), probably a residue from the O-ring and/or some lubricant. The source of metallic copper in this highly reactive zone was probably the copper mount.

D. Surface Pitting

The formation of pits into and through the downstream surface of the beryllium was found only on the type C window (see Fig. 10). It is unclear how these pits formed. They are generally located in the area where the rubber O-ring came into contact with the window surface. Also associated with this area, as explained above, is the gel. The most severe pitting was located in that area where the lower part of the SR beam intersected with the O-ring. This is also the area where deposits of elemental copper are found. One conjecture is that in this highly reactive area, very rapid rates of oxidation occured, thus eating into and through the beryllium surface. As was mentioned in the section above, the texture of the beryllium around the pits was no longer hard but had become viscous.

E. Liquid Droplets

As mentioned above, no liquids were detected on these windows. However, in a separate experiment to test protective coatings on beryllium window surfaces (to be described in a future report), liquid droplets were formed on surfaces in air in the vicinity of the SR beam. Figure 24 shows the configuration used on the X12A diagnostic beam line. The lead cover in the diagram is a 1/16" thick piece of lead sheet loosely wrapped around the volume separating the tail piece KF flange and the aluminum block. No initial attempt was made to seal any of the gaps formed in this wrapping, thus air exchange was possible in and around the covered volume. Air movement in the hutch was generated by a 590 cfm exhaust fan.

Table 3. X12A Beam Line Configuration

Ring Energy:	2.5 GeV
Ring Current:	Varied from 45-120 mA
Critical Energy:	5.070 keV
Dipole Bending Magnet (Source) Field:	1.22 Tesla
SR beam passes through:	
- two beryllium windows, total thickness	= 0.508 mm
- tantalum slits (x = 6 mm, y = 29 mm)	= 11,268 mm from source
- total path length of SR beam in air	= 237 mm
- upstream face of aluminum block	= 11,418 mm from source

After this configuration had been exposed to a white SR beam for three days, the upstream surface of the aluminum block in the area surrounding the aperture was covered by a thin layer of liquid which had coalesced into droplets in some areas. The droplets were a clear yellow in color and appeared to be reacting slightly with the surface of the aluminum. "p Hydrion Papers 1.0-2.5" (Micro Essential Laboratory, Brooklyn, New York) litmus type paper was wiped over the droplets and the color change indicated a pH of 1.0-1.5.

Subsequent to this observation the gaps in the lead wrapping were completely sealed using aluminum tape for the purposes of monitoring ozone production in this volume. The beam was run through this volume for two days during which no liquid droplets were formed (ozone concentrations within the volume were ≈ 100 ppm). The aluminum tape was then removed and after a further two days of white beam, droplets had again formed.

For analytical purposes, 15-16 $\mu\ell$ of these droplets were collected over a three day period using a Gilson P20 micropipette and dissolved into 2 ml of deionized water held in a glass vial with a plastic stopper. Analysis revealed that the liquid droplets contained nitrate. The concentration of the nitrate in the original droplets was calculated as 7.01 Molar. In view of the

fact that the pH of these droplets was between 1.0 and 1.5, the liquid formed was almost assuredly nitric acid (molarity of concentrated nitric acid is 15.8) which then reacted with the aluminum surface to form aluminum nitrate. Had this liquid formed on the surface of a beryllium window, beryllium nitrate would probably have formed. This confirms the observations of individuals in various SR facilities around the world (see Introduction).

The configuration described above indicates that a constant flow of air as well as localized production of ozone are needed to produce the nitric acid on a given surface. By sealing the volume under observation, only a finite amount of nitrogen was available (78% by volume as N_2)[2] for the production of acid particles, thus no visible deposits occured.

The health risks of and exposure limits to beryllium nitrate are similar to those detailed above for beryllium oxide.[6] Perhaps not immediately obvious when discussing the fact that nitric acid can form on surfaces adjacent to an SR beam is the possibility that acid aerosols (an inhalation hazard) might also form in the atmosphere of the hutch. McGill et al[7] state the following:

> "If the nitric oxide (a normal constituent of air) is introduced into an atmosphere containing small amounts of ozone... The reaction:
>
> $$NO + O_3 = NO_2 + O_2$$
>
> has a half-life of about 1.8 sec if both ozone and nitric oxide are present at 1 ppm. The half-life is 18 sec if both are present at 0.1 ppm... If ozone is initially in excess, ... the (above) reaction is followed by:
>
> $$2NO_2 + O_3 = N_2O_5 + O_2$$
>
> $$N_2O_5 + H_2O = 2HNO_3 \text{(nitric acid)}$$
>
> ...The equilibrium for both reactions... lies far to the right. These considerations suggest that in the presence of an excess of ozone, a large proportion of the 'oxides of nitrogen' in the atmosphere would actually be present as nitric acid vapor.

This last statement typifies the conditions prevalent around the configuration in Fig. 24.

IV. ADDENDUM

Aluminum Window Surface Deposits

As mentioned in the Introduction of this report, the use of an aluminum window is recommended downstream of a beryllium window.[1] The current NSLS design recommended for an aluminum window[8] is a sandwich consisting of two 1.3 mm thick aluminum 1100-0 apertured disks enclosing a 0.025 mm thick aluminum 5052-H34 foil (see Fig. 25). The assembly is electron beam welded and vacuum sealed by the knife edges of the beam line flange in which it is located. A new aluminum window design has been developed at the NSLS and will be implemented in the future beam lines (private communication T. Oversluizen, NSLS).

Table 4. Composition of Alloys Used in Aluminum Windows(%)[9]

AA Desig.[a]	Si[b]	Fe	Cu	Mn	Mg	Cr	Zn	Others	Aluminum
1100	1.0 (Si + Fe)		0.05-0.20	0.05	-	-	0.10	0.15	99.00
5052	0.25	0.40	0.10	0.10	2.2-2.8	0.15-0.35	0.10	0.15	Remainder

a. Aluminum Association Designation.
b. Composition in % maximum unless shown as a range or a minimum.

When exposed to white SR beam, the downstream face of the aluminum window reacts with the air and locally formed ozone producing white crystals on the window surfaces. Such crystals were collected from an aluminum window on the X19A beam line by gently brushing the surface of the window with a camels hair brush. The majority of the crystals were from the surface of the 1100-0 apertured disk.

Energy dispersive x-ray spectrometry (EDS) revealed the presence of aluminum as well as trace amounts of iron (see Fig. 26). As can be seen from Table 3 above, iron is a contaminant of aluminum 1100-0. Electron diffraction pattern (see Fig. 27) calculations revealed that the majority of the crystalline material is metallic aluminum and that some aluminum oxide phase is also present which is what would be expected on this surface. The EELS plot (see Fig. 28) reveals the oxygen k-absorption edge (532 eV) as well as possible ℓ-absorption edge features of Al(78.7 eV) and Si(97.9 eV), silicon also being a contaminant of aluminum 1100-0. The latter two edge values do not exactly match values available in the literature due to a possible scaling factor shift at this end of the scan (personal communication R. Sabatini). This reinforces the electron diffraction analysis showing the presence of aluminum oxide.

While no surface degradation was observed by the naked eye on the aluminum foil of this particular window assembly, aluminum windows on the other beam lines have been known to develop vacuum leaks. Some of these leaks were traced to mechanical damage of the foil and/or the weld of the assembly itself. However, with the presence of severe surface oxidation of the foil due to an intense white SR beam, it is possible that surface degradation may cause a vacuum leak.

Acknowledgements

This paper could never have been written without the generous assistance and ideas of the following people: Paul Klotz and staff (DAS) for wet chemical analysis; Robert Sabatini (DAS) for chemical and structural analysis; staff members and users in the National Synchrotron Light Source Department for supplying many of the materials needed for analysis and for supplying historical information.

V. BIBLIOGRAPHY

1. Thomlinson, W. April 8, 1981. Be Windows on X-Ray Beam Lines at NSLS. NSLS Bulletin 81-6, 6pp.

2. CRC Handbook of Chemistry and Physics - 66th Edition. 1985. Ed. by R.C. Weast. CRC Press, Inc., Boca Raton, Florida. pp.B9-10, B77, F156.

3. Kirk-Othmer Encyclopedia of Chemical Technology - Volume 3. 1978. John Wiley & Sons, N.Y. pp.803-829.

4. Joint Committee on Powder Diffraction Standards. 1981 series. International Center for Diffraction Data, Swarthmore, Pa.

5. Moeller, T. 1952. Inorganic Chemistry: An Advanced Textbook. John Wiley & Sons, Inc., N.Y. p.858.

6. Sax, N.I. 1984. Dangerous Properties of Industrial Materials - Sixth Edition. Van Nostrand Reinhold Company, New York p.424.

7. MaGill, P.L., F.R. Holden and C. Ackley (eds.). 1956. Air Pollution Handbook. McGraw-Hill Book Company, N.Y. pp.3-18 to 3-20.

8. Schuchman, J.C. 1983. Final Design and Status of the NSLS Vacuum System. J. Vac. Sci. Technol. A1(2): 196-200.

9. The Aluminum Association, Inc. 1976. Aluminum Standards and Data. pp. 92, 93, 99.

10. Webster, D. and G.J. London (eds.). 1979. Beryllium Science and Technology - Vol. 1. Plenum Press, N.Y. 330 pp.

VI. FIGURES

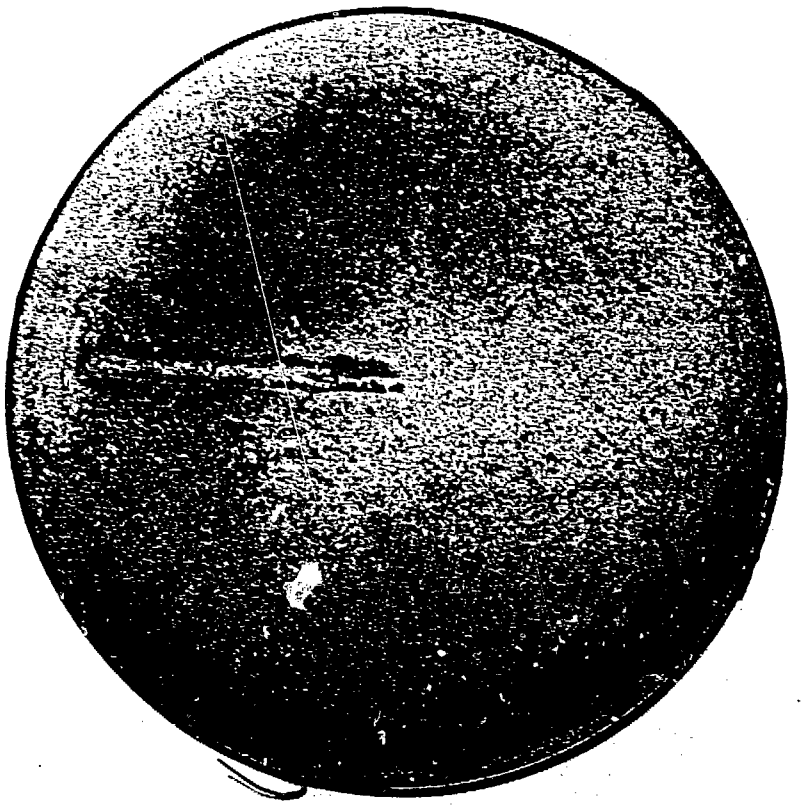

Fig. 1. Type A beryllium window - full view (diam. = 1.5"); powder and lacquer deposits.

Fig. 2. Type A beryllium window - 25x bright field image of surface deposit seen in Fig. 1.

Fig. 3. Type A beryllium window - full view (diam. = 1.5"); lacquer deposit only.

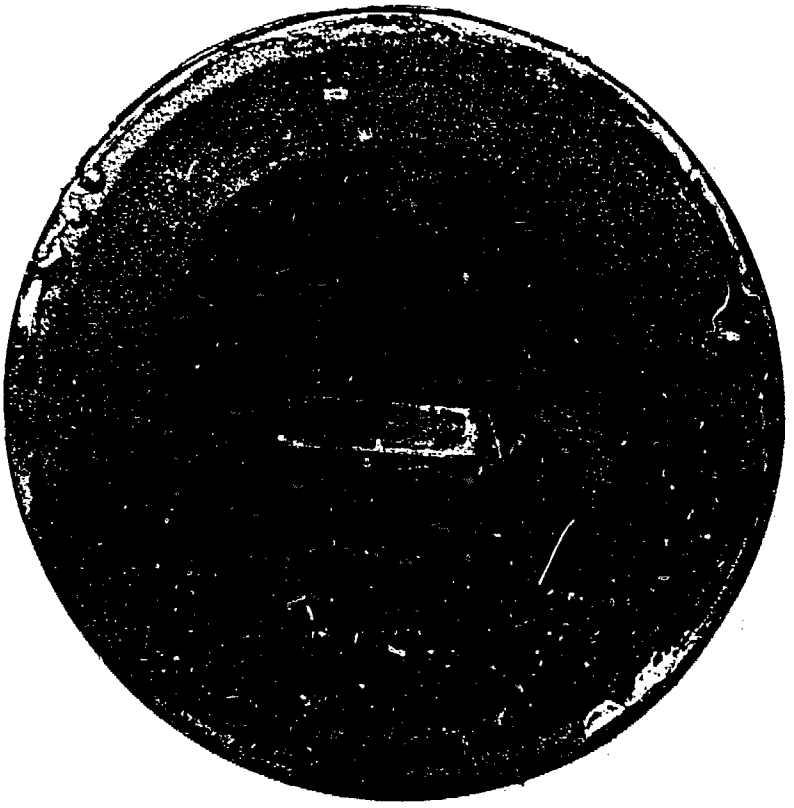

Fig. 4. Type B beryllium window - full view (diam. = 1.5"); white powder surface deposit.

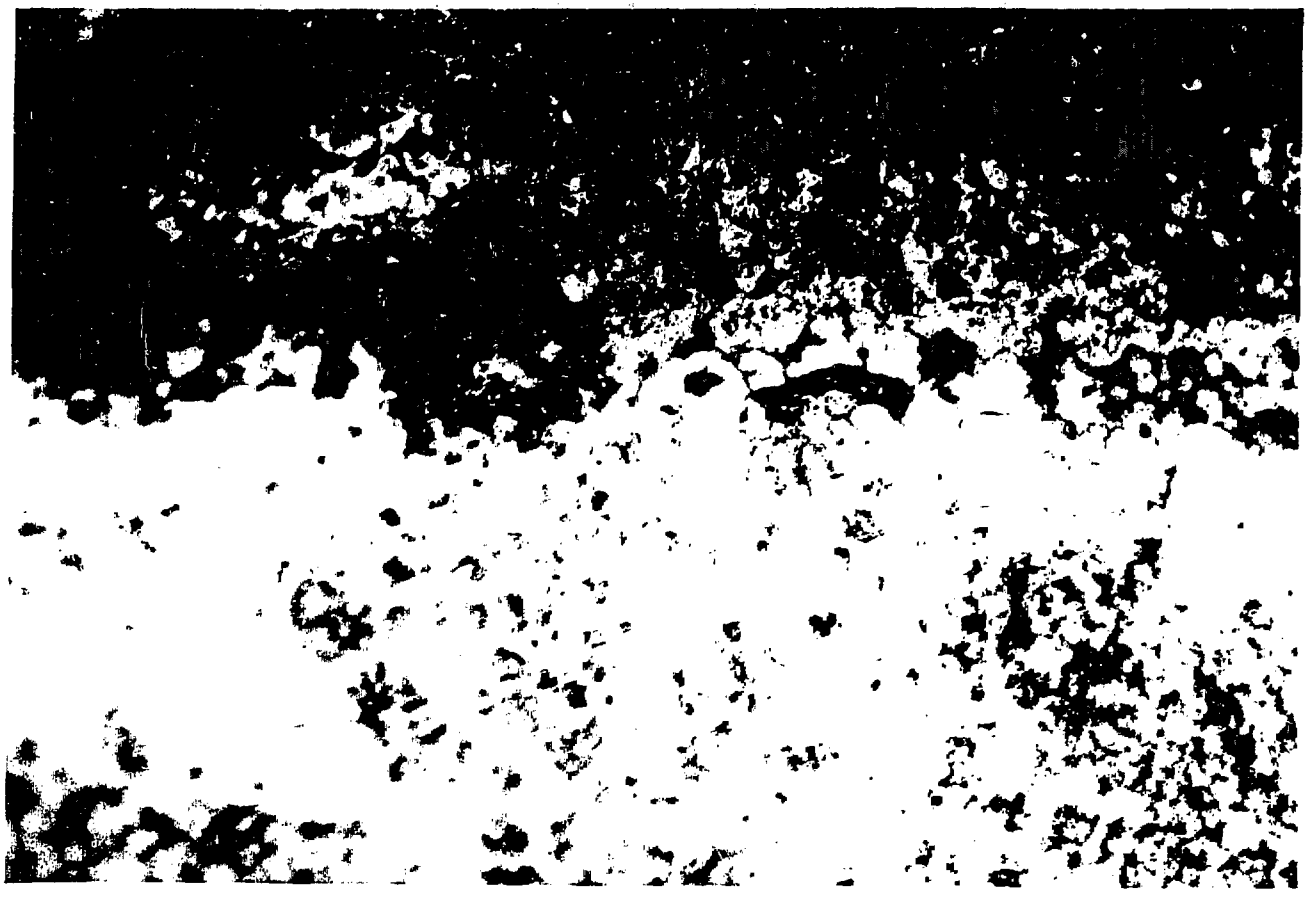

Fig. 5. Type B beryllium window - 80x bright field image of powder deposit edge seen in Fig. 4.

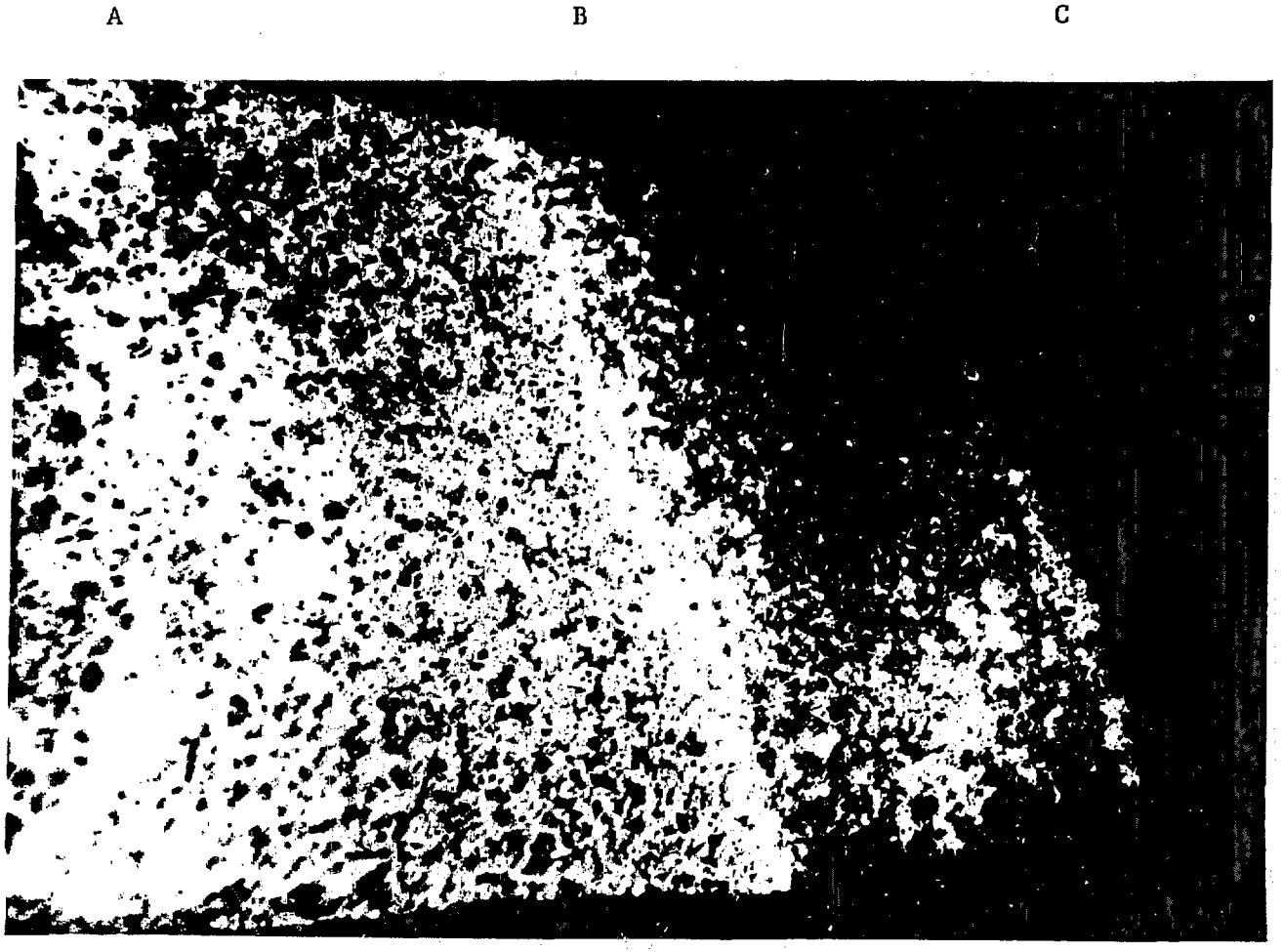

Fig. 6. Type B beryllium window - 25x bright field image of powder deposit ends seen in Fig. 4. A, B, and C indicate positions of three separate horizontal aperture openings.

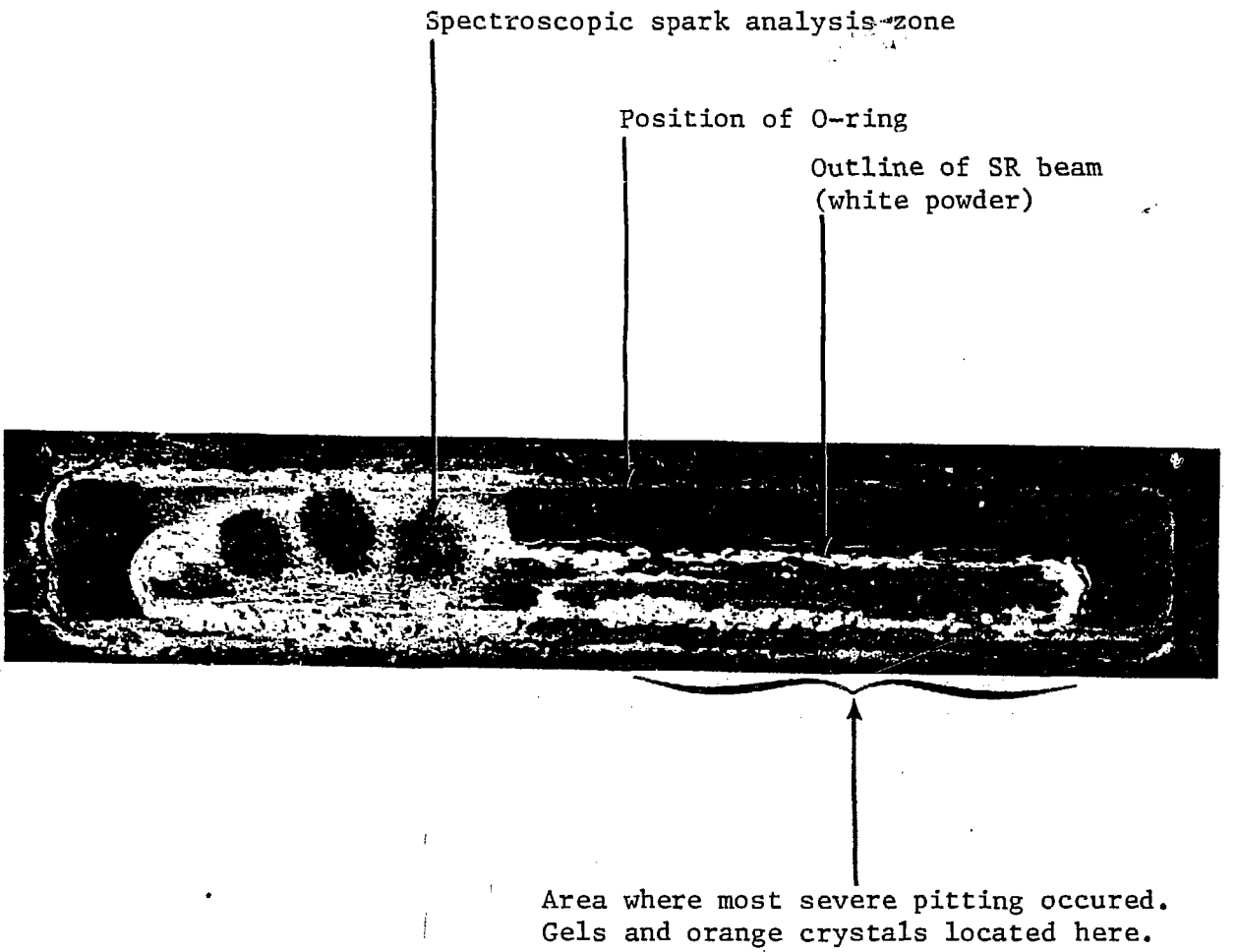

Fig. 7. Type C beryllium window - full view (size = 4.0" x 0.75"); various types of deposits.

Fig. 8. Type C beryllium window - 80x bright field image of blue/green gel deposit.

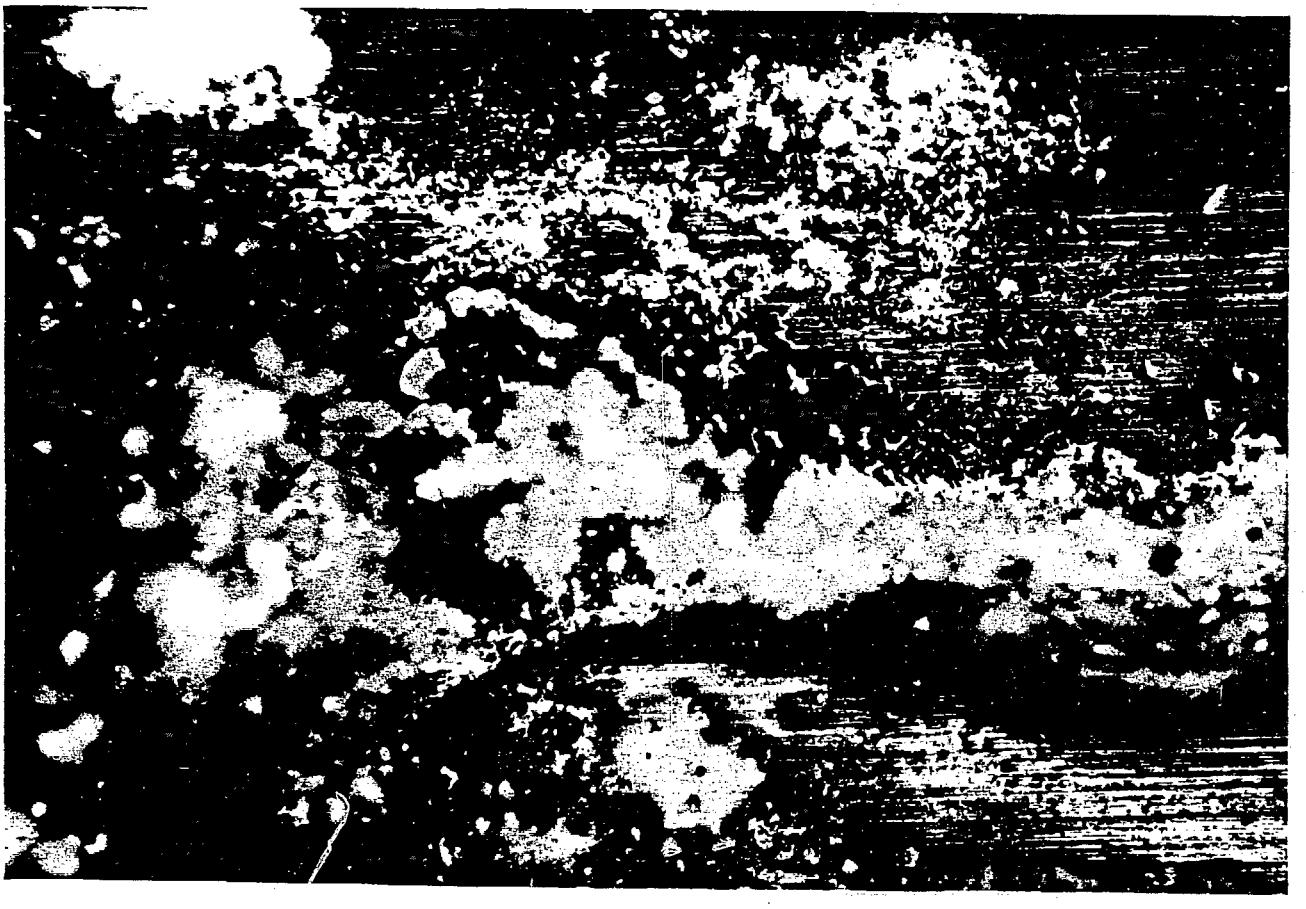

Fig. 9. Type C beryllium window - 25x bright field image of white gel deposit.

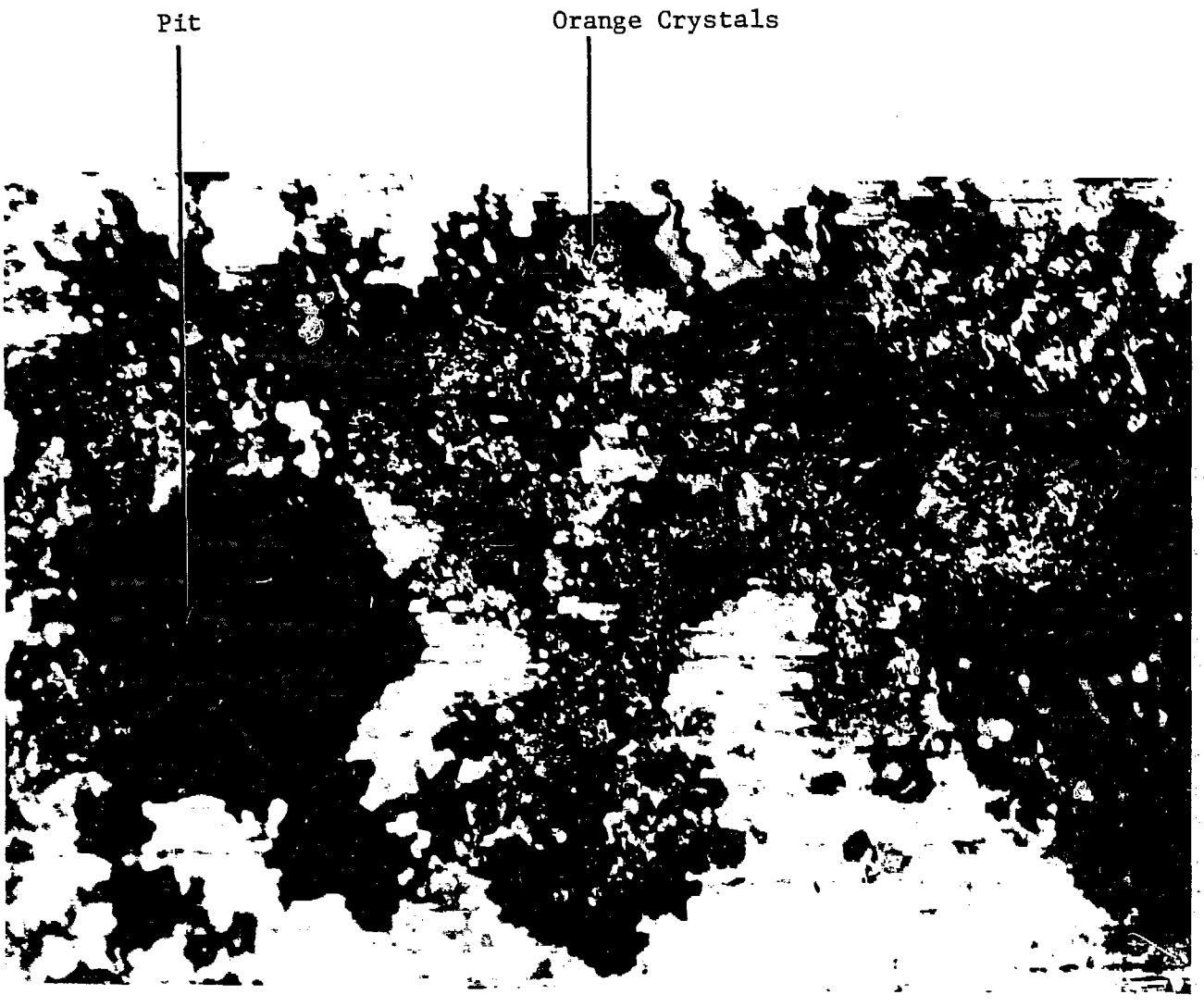

Fig. 10. Type C beryllium window - 80x bright field image of surface pitting and orange-colored crystals.

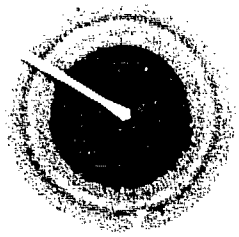

Fig. 11. Electron diffraction pattern of white powder - BeO.

Fig. 12. Electron diffraction pattern calculations determining presence of BeO in white powder.

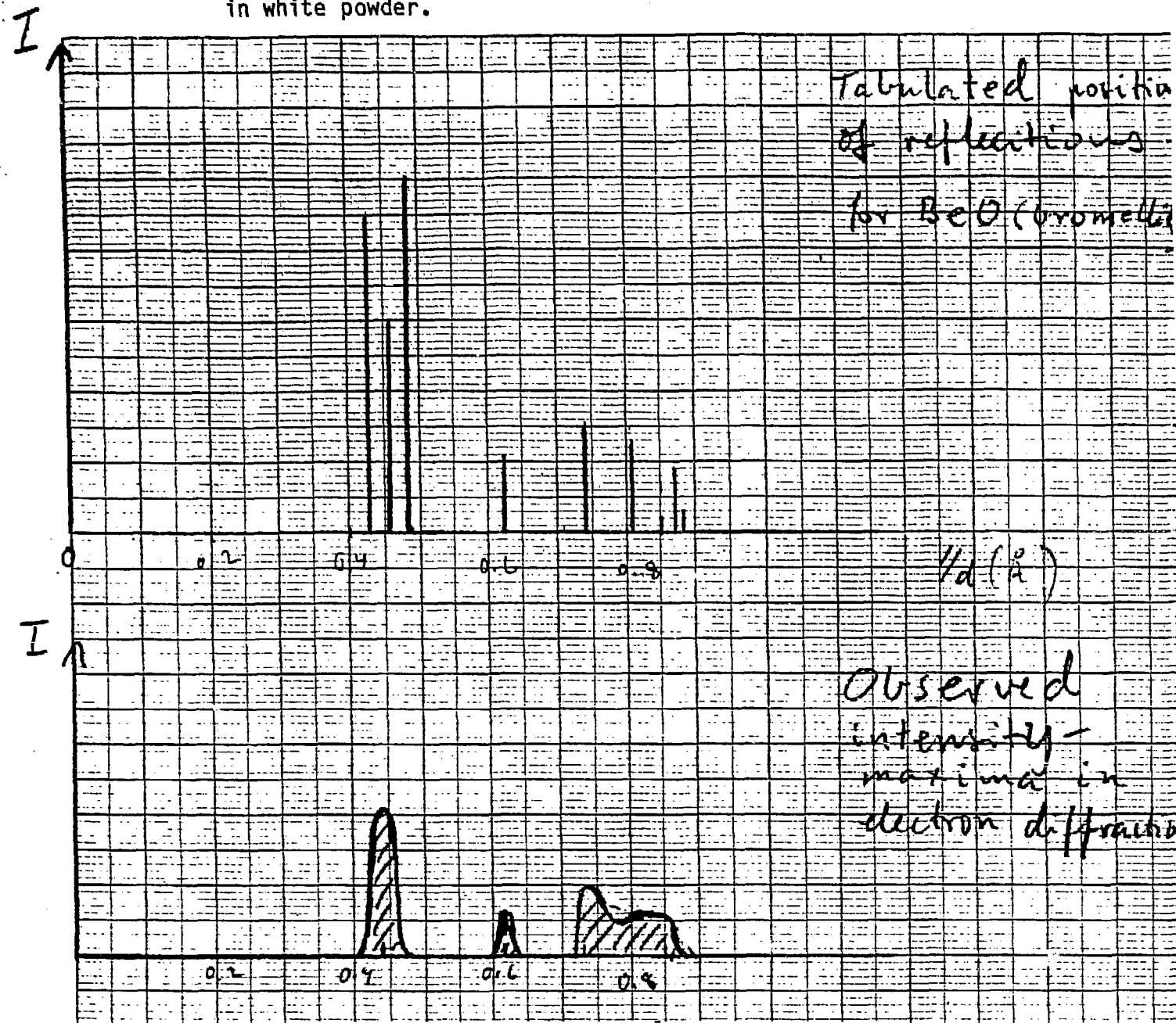

4-0843 MINOR CORRECTION

d (4-0843)	2.08	2.34	2.19	2.337
I/I$_1$ (4-0843)	100	91	61	91

BeO

BERYLLIUM OXIDE (BROMELLITE)

Rad. $CuK\alpha_1$ λ 1.5405 Filter Ni
Dia. Cut off Coll.
I/I$_1$ G. C. DIFFRACTOMETER d meas. by I
Ref. SWANSON AND TATGE, J. RES. NBS (1951)

Sys. HEXAGONAL S.G. C^4_{6v} - $P6_3mc$
a_o 2.6979 b_o a_o 4.380 Å C 1.625
α β γ Z 2 D_x 3.009
Ref. Ibid.

ε ω $\alpha=\beta$ 1.719 γ 1.733 Sign +
2V D mp Color WHITE
Ref. D_x

[4] ZACHARIASEN, Z. PHYS. CHEM. 119, 201-13 (1926)
SPECTROGRAPHIC ANALYSIS SHOWS 0.03% Al, <0.01% EACH OF Ca, Fe, Mn, Si, AND TRACES OF Cu, Pb, Sn
AT 26°C
TO REPLACE 1-1258, 3-0826, 3-0928, 3-1035

d Å	I/I$_1$	hkl	d Å	I/I$_1$	hkl
2.337	91	100			
2.199	61	002			
2.061	100	101			
1.598	22	102			
1.349	29	110			
1.238	24	103			
1.1682	4	200			
1.1482	16	112			
1.1281	5	201			
1.0958	<1	004			
1.0308	3	203			
0.9920	<1	104			
.9118	10	202			
.8832	4	210			
.8457	5	211			
.8496	2	114			
.8199	14	105			
.8179	8	212			

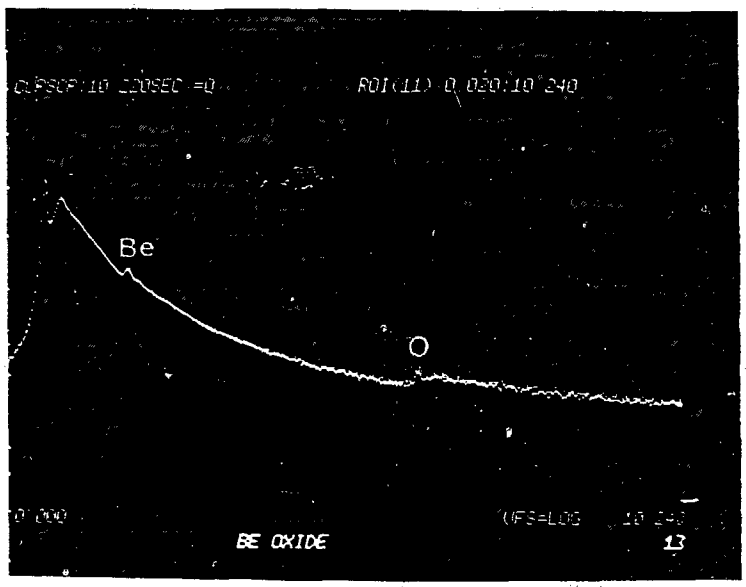

Fig. 13. Logarithmic plot of electron energy loss spectroscopy (EELS) showing presence of beryllium and oxygen in white powder.

Fig. 14. EELS plot showing beryllium (~ 111 eV) and oxygen (~ 532 eV) k absorption edges in white powder.

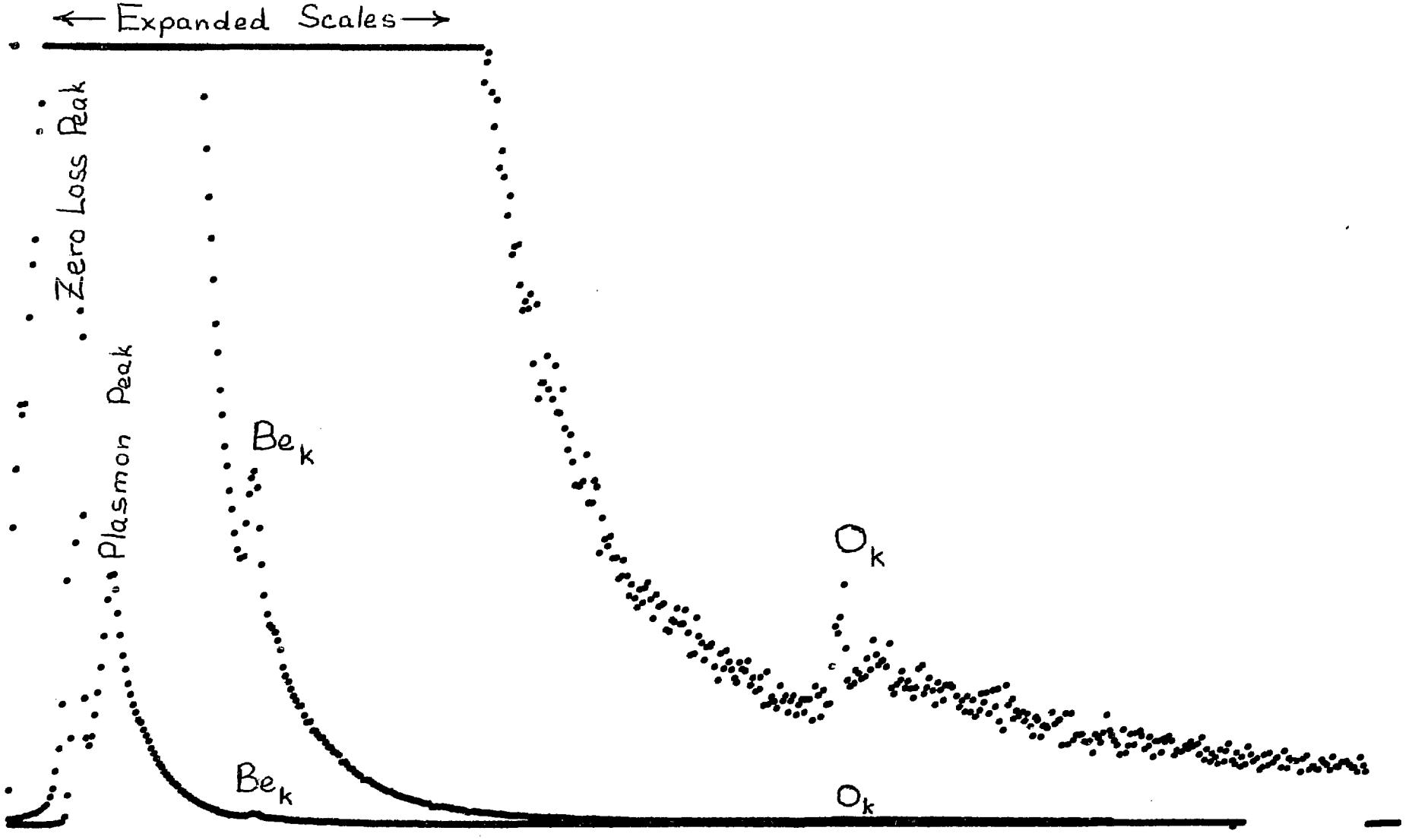

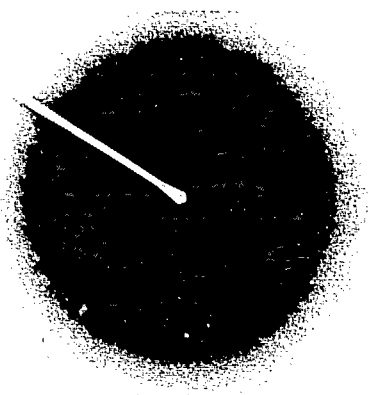

Fig. 15. Electron diffraction pattern of white gel - amorphous carbon.

"Clear Gel"

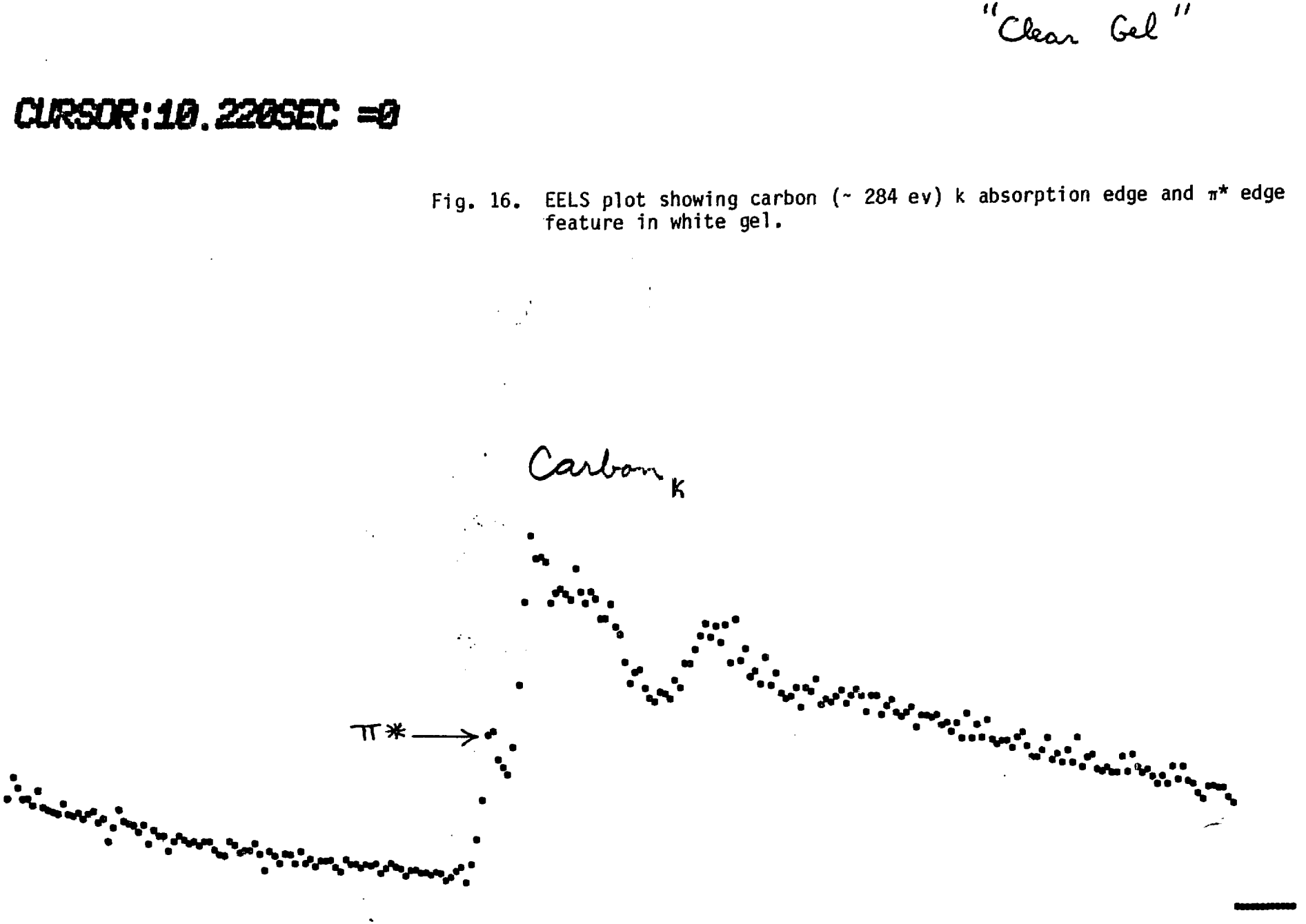

Fig. 16. EELS plot showing carbon (~ 284 ev) k absorption edge and π* edge feature in white gel.

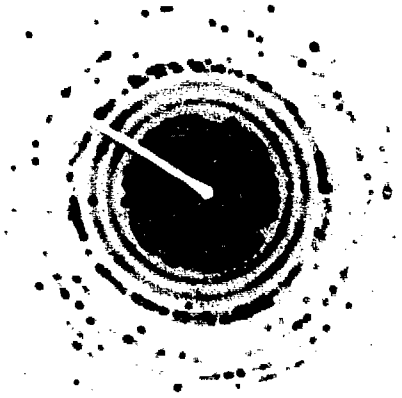

Fig. 17. Electron diffraction pattern of blue/green gel - copper and cupric oxide (Cu_2O).

Fig. 18. Electron diffraction pattern calculations determining presence of Cu and Cu_2O in blue/green gel.

Tabulated Electron Diffraction Analysis

"Blue Gel" + "Orange XLS"

Measured →	d Å	Cu_2O (Ref)	Cu (Ref)
11.5 mm →	3.07 Å	3.02	
14.0 mm →	2.52 Å	2.47	
16.7 mm →	2.06 Å		2.09
19.2 mm →	1.79 Å		1.81
23.2 mm →	1.52 Å	1.51	
27.3 mm →	1.28 Å	1.29	
32.5 mm →	1.06 Å		1.09

Cu

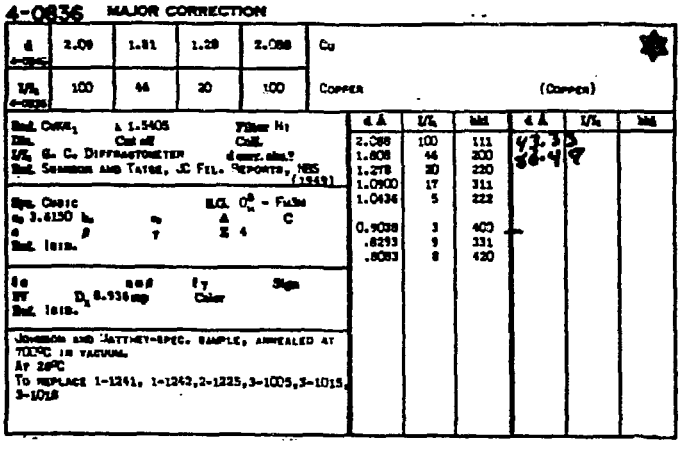

4-0836 MAJOR CORRECTION

d	2.09	1.81	1.28	2.088	Cu
I/I$_1$	100	46	20	100	COPPER (COPPER)

d Å	I/I$_1$	hkl	d Å	I/I$_1$	hkl
2.089	100	111	43.35		
1.808	46	200	50.49		
1.278	20	220			
1.0900	17	311			
1.0436	5	222			
0.9038	3	400			
.8293	9	331			
.8083	8	420			

Johnson and Matthey-spec. sample, annealed at 700°C in vacuum.
At 26°C
To replace 1-1241, 1-1242, 2-1225, 3-1005, 3-1015, 3-1018

Cu_2O

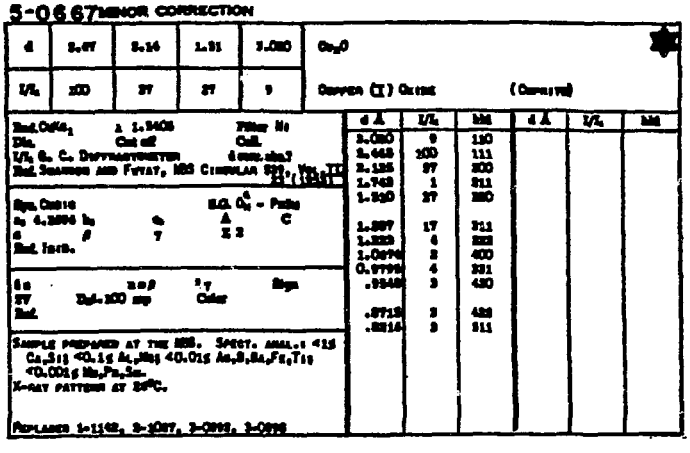

5-0667 MINOR CORRECTION

d	3.07	2.14	1.51	1.030	Cu_2O
I/I$_1$	100	57	57	9	Copper (I) Oxide (Cuprite)

d Å	I/I$_1$	hkl	d Å	I/I$_1$	hkl
3.080	9	110			
2.465	100	111			
2.135	57	200			
1.748	1	211			
1.510	27	220			
1.397	17	311			
1.233	4	222			
1.0674	2	400			
0.9799	4	331			
.9548	3	420			
.8715	3	422			
.8216	3	511			

Sample prepared at the NBS. Spect. anal.: 41% Ca, 51% <0.1% Al, Mg; 40.01% As, B, Ba, Fe, Ti; <0.001% Mn, Pb, Sn.
X-ray pattern at 26°C.

Replaces 1-1142, 2-1017, 3-0915, 3-0916

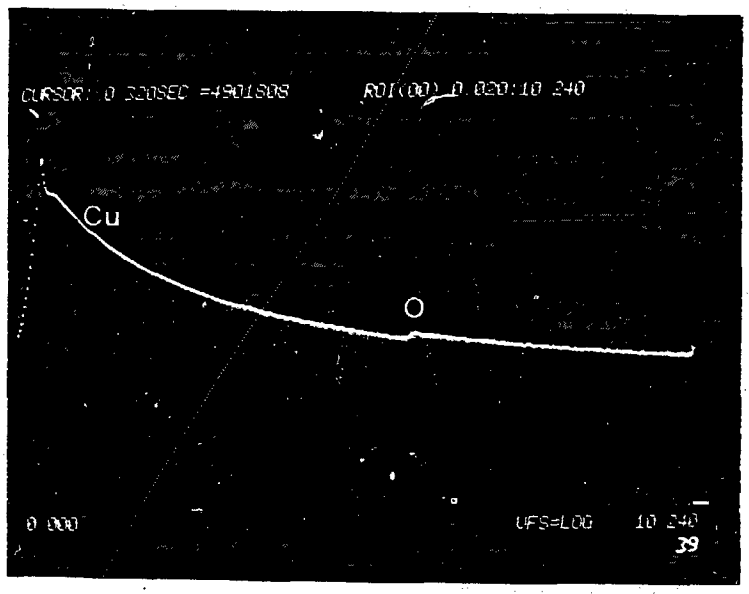

Fig. 19. Logarithmic plot of EELS analysis showing presence of Cu and O in blue/green gel.

Fig. 20. EELS plot showing copper (~ 121 eV) and oxygen (~ 540 eV) M_1 and k absorption edges, respectively, in blue/green gel.

"Blue Gel"
#1
100 s/scan
1 ev/ch

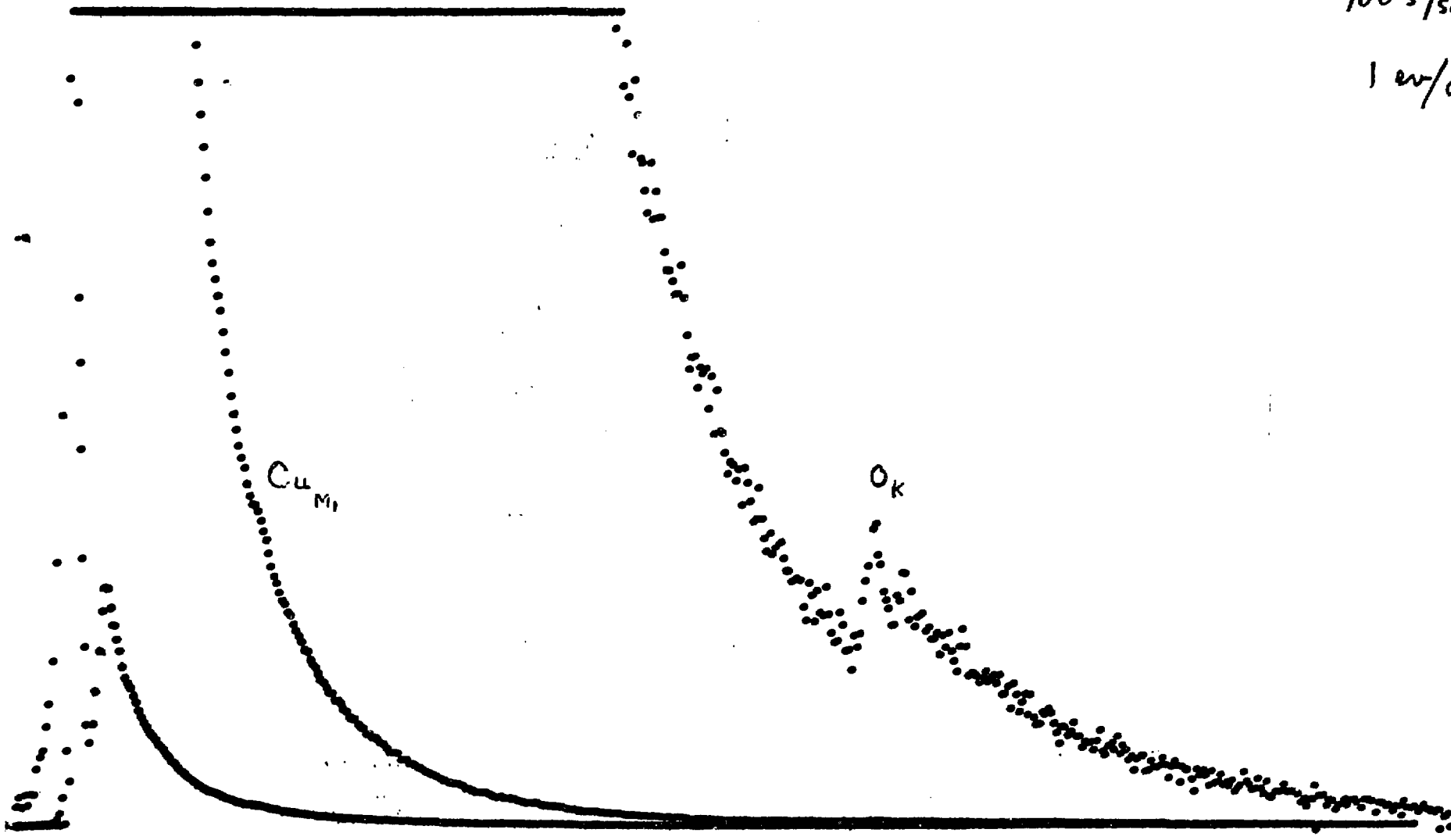

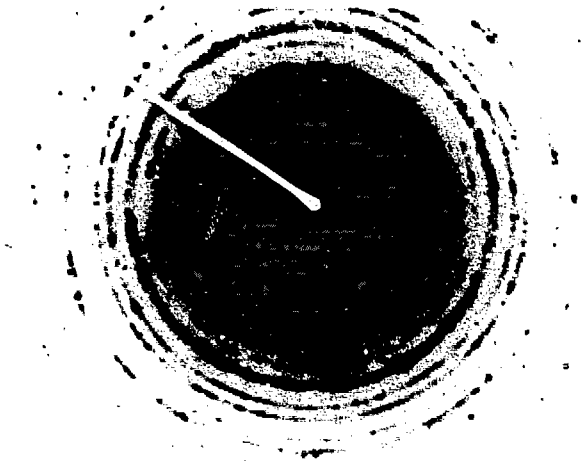

Fig. 21. Electron diffraction pattern of orange crystals - Cu and Cu_2O.

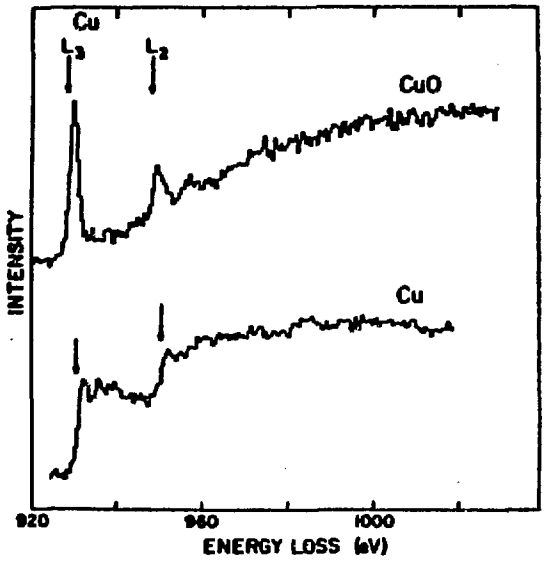

FIG. 6. L_{23} edge spectra from Cu and CuO extending ~100 eV above threshold.

Fig. 22. EELS plot showing copper L_3 (~ 931 eV) and L_2 (~ 951 eV) absorption edges in orange crystals.

orange xls

Cu + Cu O

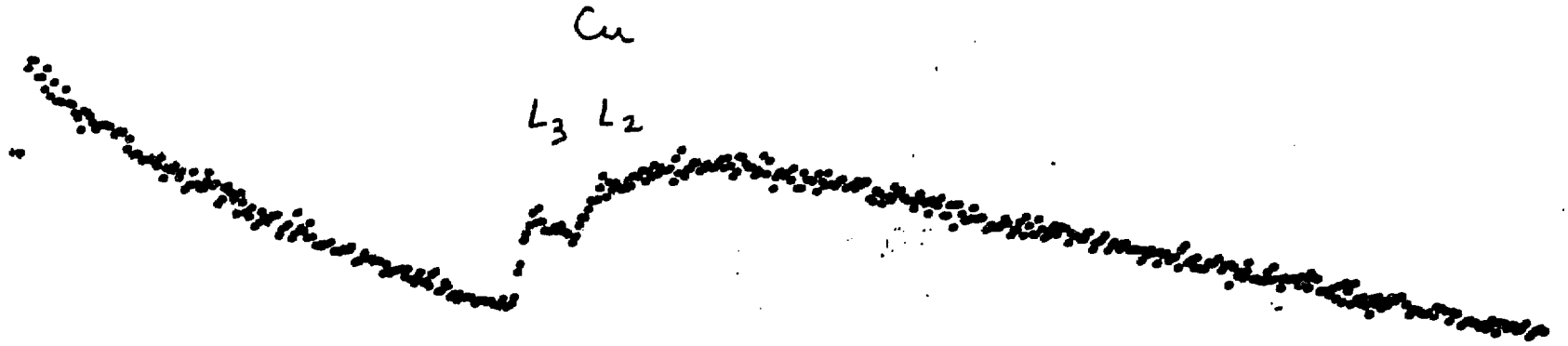

Fig. 23. EELS plot showing carbon (~ 280 eV) k absorption edge in orange crystals.

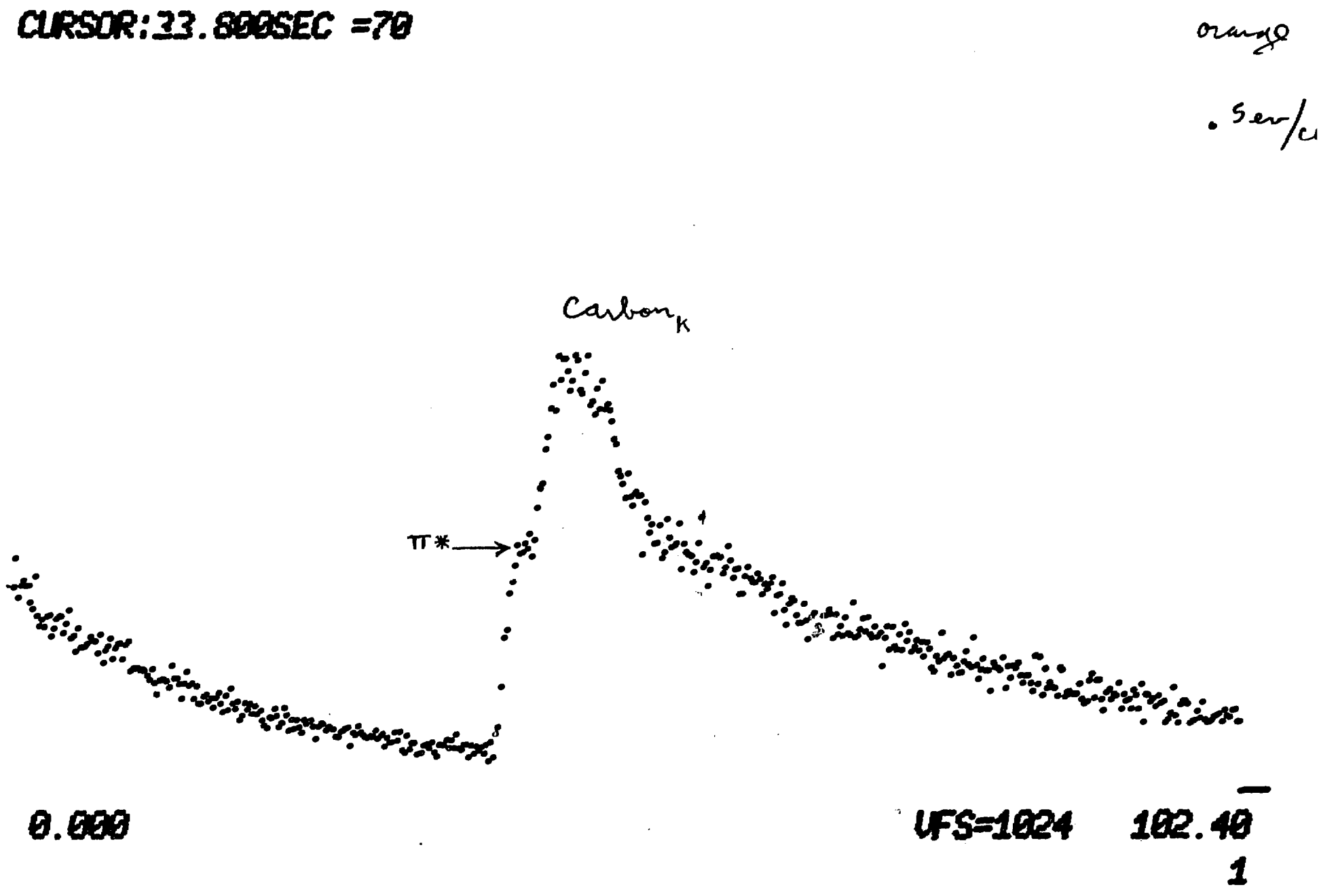

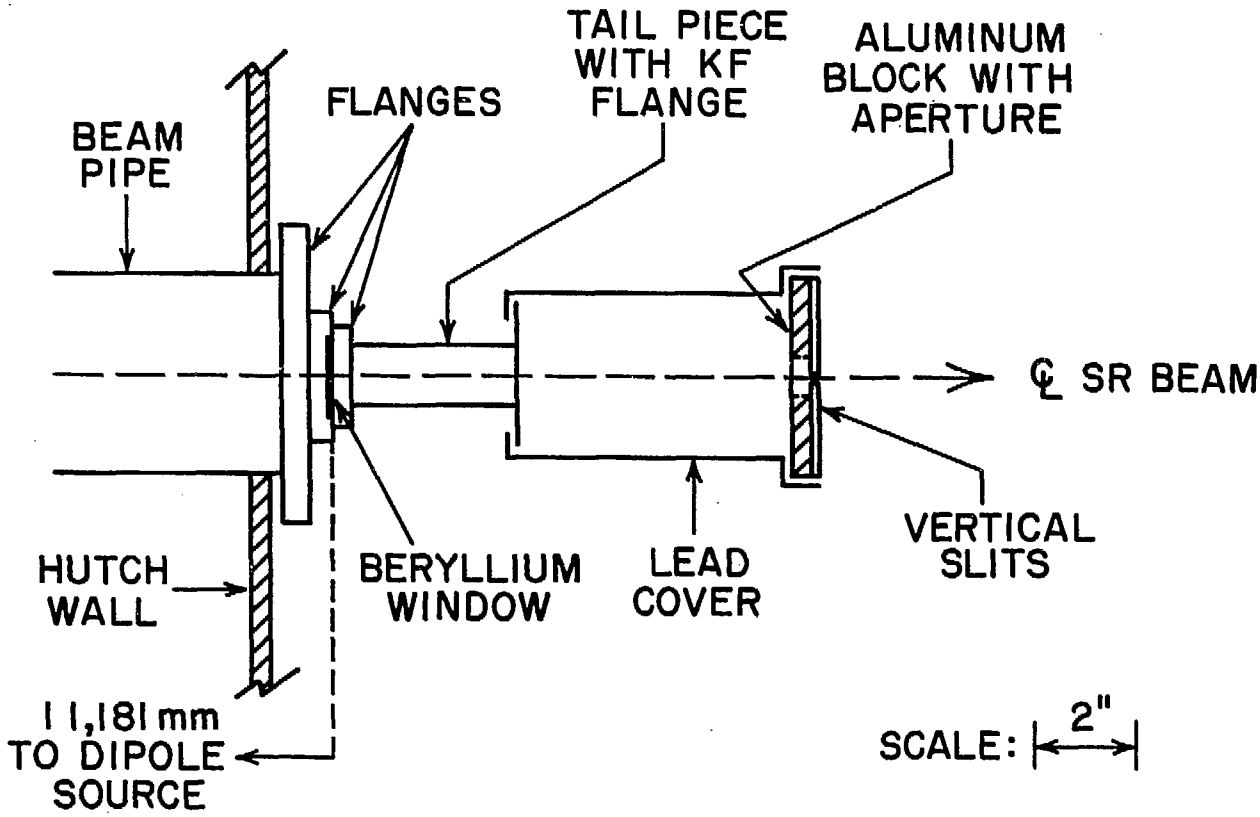

Fig. 24. Diagram of beam line configuration during generation of nitric acid droplets.

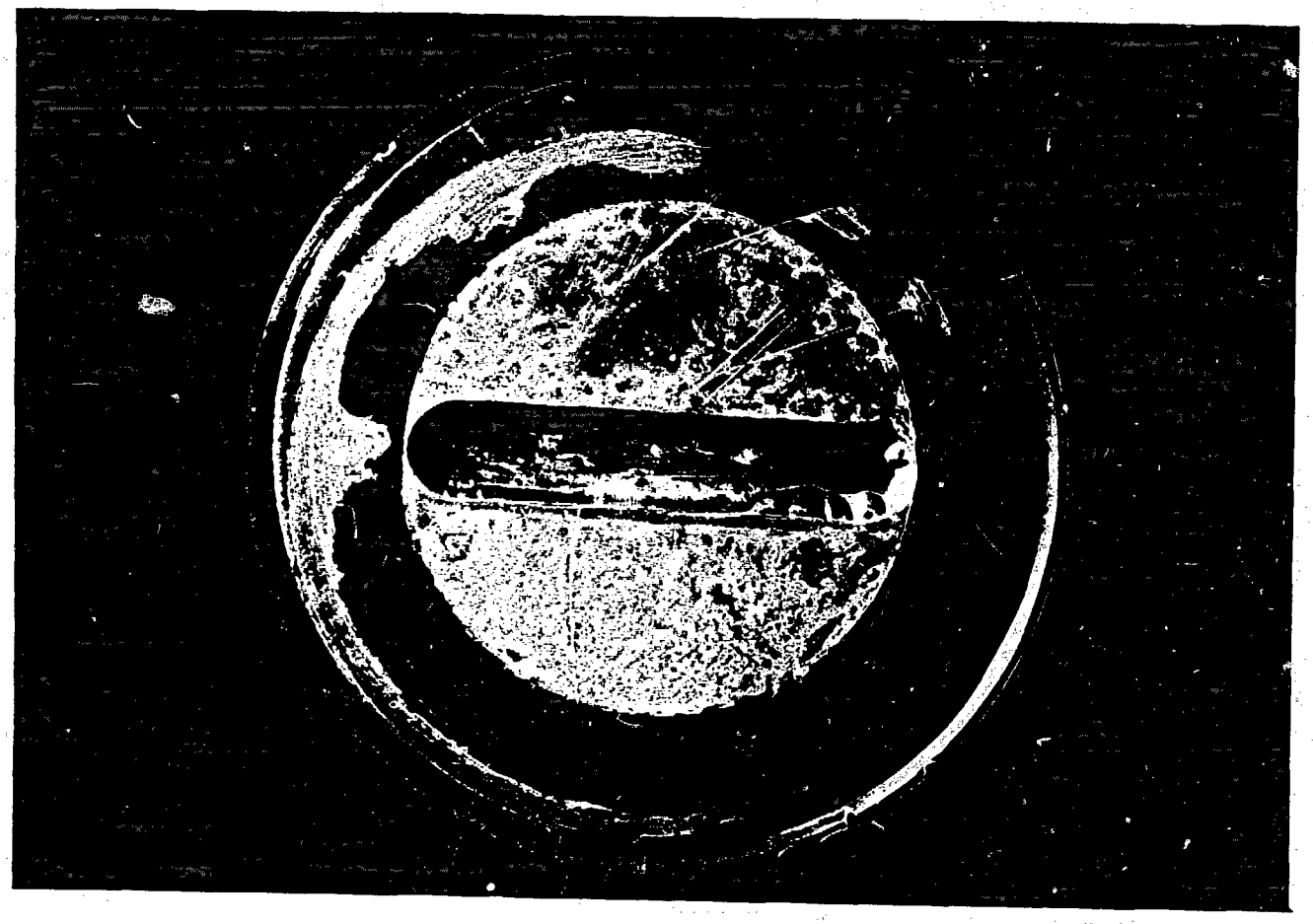

Fig. 25. Aluminum window - full view (diam. = 82.4 mm); powder deposits.

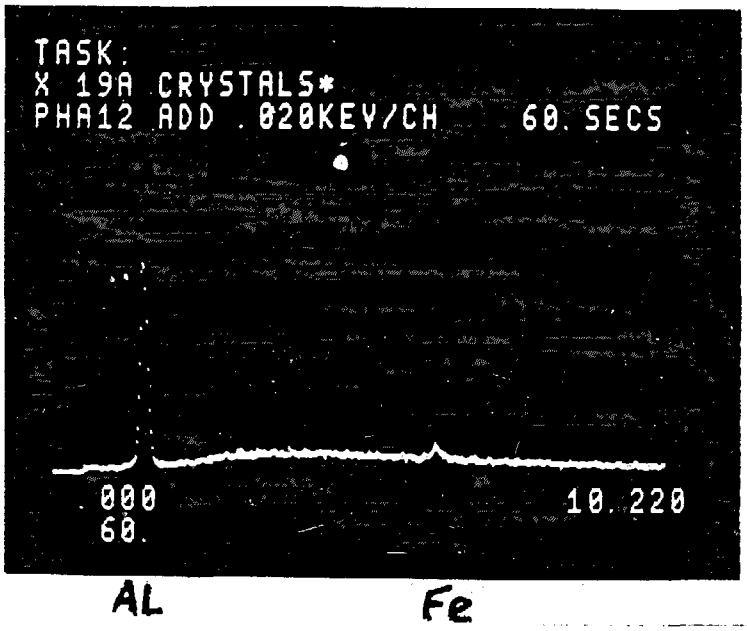

Fig. 26. Energy dispersive x-ray spectroscopy plot of crystals on surface of aluminum window showing aluminum and iron (trace) peaks.

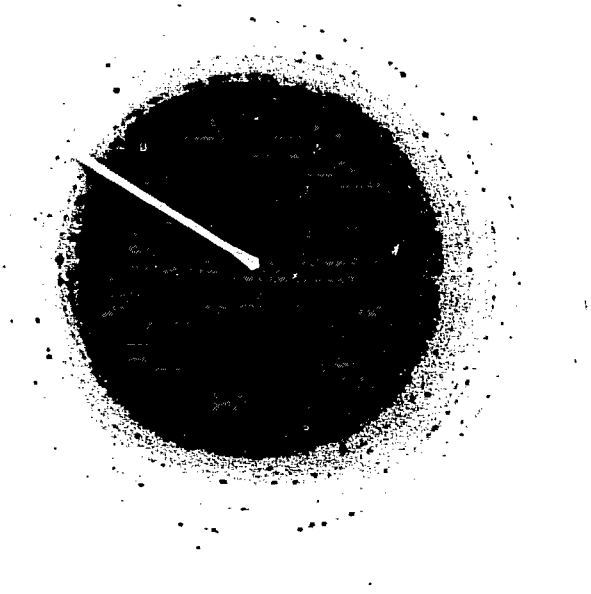

Fig. 27. Electron diffraction pattern of aluminum window surface crystals showing presence of metallic aluminum and aluminum oxide.

Fig. 28. EELS plot of aluminum window surface crystals showing presence of oxygen k absorption edge (532 eV) and ℓ absorption edge features of aluminum (78.7 eV) and silicon (97.9 eV).

2 ev/ch